Instrument for accurate measurement of high alternating current impedances

ARTICLE *in* ANALYTICAL CHEMISTRY · JUNE 1986

Impact Factor: 5.64 · DOI: 10.1021/ac00298a052

3 AUTHORS, INCLUDING:

Karl Cammann
University of Münster

cisely and without reference to a calibration curve. The interference of the system may be regarded as similar to that of batchwise argentimetric titration. For natural water analysis, the most probable interference comes from bromide, and the error caused by the presence of bromide was less than 2% (*13*). The response time may be shortened by using a high flow rate and/or miniaturizing the whole system. If this system is perfectly modified to be portable, it must be used more usefuly for continuous monitoring of a stream water and for obtaining the daily variation profile of concentration of chloride.

Registry No. H_2O, 7732-18-5; Cl^-, 16887-00-6.

LITERATURE CITED

(1) Hulanicki, A.; Trojanowicz, M. *Ion-Sel. Electrode Rev.* **1979**, *1*, 207–248.
(2) Mansell, R. S.; Elzeftawy, A. *Soil Sci. Soc. Am. Proc.* **1972**, *36*, 378–380.
(3) Tomlinson, K.; Torrance, K. *Analyst (London)* **1977**, *102*, 1–8.
(4) Trojanowicz, M.; Lewandowski, R. *Fresenius' Z. Anal. Chem.* **1981**, *308*, 7–10.
(5) Hara, H.; Wakizaka, Y.; Okazaki, S. *Analyst (London)* **1985**, *110*, 1087–1090.
(6) Fehér, Zs.; Nagy, G.; Tóth, K.; Pungor, E. *CRC Crit. Rev. Anal. Chem.* **1983**, *14*, 175–230.
(7) Fleet, B.; Ho, A. Y. W. *Talanta* **1973**, *20*, 793–798.
(8) Fleet, B.; Ho, A. Y. W. *Anal. Chem.* **1974**, *46*, 9–11.
(9) van Osch, G. W. S.; Griepink, B. *Fresenius' Z. Anal. Chem.* **1977**, *284*, 267–271.
(10) Nagy, G.; Fehér, Zs.; Tóth, K.; Pungor, E. *Anal. Chim. Acta* **1977**, *91*, 97–106.
(11) Růžička, J.; Hansen, E. H.; Mosbaek, H. *Anal. Chim. Acta* **1977**, *92*, 235–249.
(12) Trojanowicz, M. *Anal. Chim. Acta* **1980**, *114*, 293–301.
(13) Hara, H.; Okazaki, S. *Analyst (London)* **1984**, *109*, 1317–1320.
(14) Cattrall, R. W.; Kwok-Tai, Fong *Talanta* **1978**, *25*, 541–543.
(15) Freiser, H.; Fernand, Q. *Ionic Equilibria in Analytical Chemistry*; Wiley: New York, 1963.
(16) Forsythe, G. E.; Malcolm, M. A.; Moler, C. B. *Computer Method for Mathematical Computation*; Prentice-Hall: Englewood Cliffs, NJ, 1977.
(17) Gen, M.; Ida, K. *Programs of Scientific Calculations for a Personal Computer*; Kogaku tosho shuppan: Tokyo, 1983; p 109.
(18) Horvai, G.; Pungor, E. *Anal. Chim. Acta* **1980**, *116*, 87–92.

RECEIVED for review June 25, 1985. Accepted December 31, 1985.

Instrument for Accurate Measurement of High Alternating Current Impedances

Sheng-Luo Xie,[1] Bernhard Obert, and Karl Cammann*

Department of Analytical Chemistry, University of Ulm, D-7900 Ulm, Federal Republic of Germany

An instrument based on a low-cost lock-in amplifier and homemade components for accurate measurement of high ac impedances has been developed. The construction of the circuitry, including application of a guard technique, eliminates the effect of stray capacitances in the complete system to less than 0.8 pF. The results of measurements on dummy cells consisting of a 100-MΩ resistor shunted by a 10-pF capacitor or a 100-kΩ resistor shunted by a 10-nF capacitor were in excellent agreement with the certified values. The results of measurements on an actual electrochemical cell containing a K^+-selective PVC membrane were found to be close to the results obtained by other researchers.

The application of the alternating current impedance methods for the investigation of electrochemical phenomena has expanded rapidly over the past two decades (*1–4*). This method has been used to ascertain reaction mechanisms and the structure of the double layer, including the measurement of kinetic parameters (transfer coefficients, exchange current densities, heterogeneous rate constants, etc.). For example, by use of complex impedance spectra for the analysis of electrochemical reactions, some information concerning the rates of ion transfer across the interface under study, i.e., between the ion-selective membrane and the adjacent solution or between the interface of two immiscible electrolyte solutions, can be obtained.

So far, several methods for determining the ac impedance at different frequencies for electrochemical equivalent circuit description exist. (1) The ac bridge method, developed early, is precise but rather inconvenient and very time-consuming. (2) Using phase-sensitive lock-in amplifiers, some nonbridge instruments employ a sine wave reference, and phase-sensitive detection is accomplished by a correlation technique (*5*, *6*), but these instruments are sophisticated and very expensive. (3) "Direct" methods such as Lissajous figures method with an X–Y recorder are often used for impedance measurements at lower frequencies (below 1 Hz). (4) Some low-cost instruments recently introduced, such as the battery-operated impedance spectroter (*7*), are not suitable for high ac impedance measurements.

In general, commercial impedance-measuring instruments (lock-in principle) are available only for the reliable measurement of circuits with low ohmic resistances. In this paper, the construction of an instrument for highly accurate measurements of circuits with very high ohmic components is described based on a low-cost lock-in amplifier and homemade components. This constructon eliminates almost completely the problem of stray capacitances and the capacitance of circuit critical points vs. earth (*8*). Thus this instrumental setup for high ac impedance measurements allows highly precise measurements. This is absolutely essential if small charge transfer resistances are to be measured besides the high ohmic resistance of an ion-selective bulk membrane, for example.

CIRCUIT DESCRIPTION

For high ac impedance measurements, in particular for large resistances and small capacitances, the limitation in upper frequency is controlled by the transient response of the circuit and by the bandwidths of the amplifier employed, in which the effect of stray capacitances and the capacitances of the circuit critical points vs. earth are serious problems. In the circuit design we took measures to overcome this problem. The circuit diagram of the complete instrument is shown in Figure 1. A sine alternating voltage from a signal generator (Feedback Instruments Limited FG 601 type, output impedance 600 Ω, sine distortion less than 0.6% at 1 kHz) is derived via a divider network (1 kΩ/5

[1] Visiting researcher (Humboldt Fellow) from the Chemistry Department of Wuhan University, Wuhan, People's Republic of China.

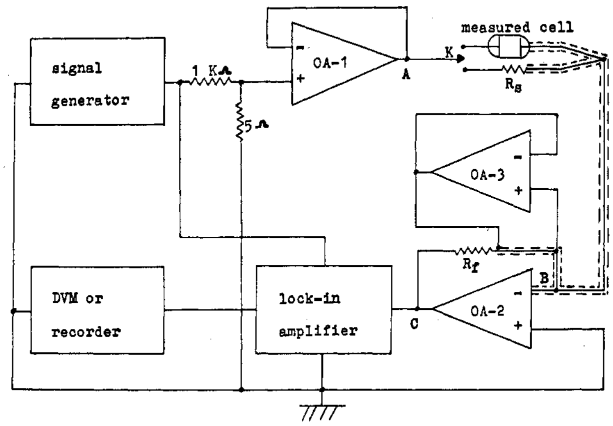

Figure 1. Circuit diagram of the instrument for measurement of high ac impedance: OA-1, PIM OP-07; OA-2, AD 515KH; OA-3, μA 748; R_s, standard resistor; R_F, feedback (measuring) resistor.

Ω in which the 1-kΩ resistor is composed of several smaller resistors in series). A check indicated that there is not any phase shift. The signal is then fed to a voltage follower composed of operational amplifier OA-1 (PIM OP-07, low noise). Because the OA-1 has large open-loop gain and high input impedance and is connected in a negative feedback mode, the result is the very low output impedance of the voltage follower, thus leading to an elimination of the effect of the frequency-limiting capacitance of point A vs. earth. Then the signal is fed to the cell whose impedance is measured or to the standard resistor, R_s. The output current from the measured cell or from R_s is derived via an $I-V$ (current–voltage) converter composed of operational amplifier OA-2 (AD 515 KH, low noise, FET input electrometer operational amplifier). In the same way, the output impedance of the $I-V$ converter is also very low, eliminating the problem of the stray capacitance of point C vs. earth. On the feedback resistor (current-measuring resistor), R_F, of the $I-V$ converter, the output current, $\tilde{I}$, from the measured cell or from the standard resistor, R_s, produces an output voltage, $\tilde{V}$, and there is

$$\tilde{V} = -\tilde{I}R_F \qquad (1)$$

This voltage, $\tilde{V}$, as the input signal is fed to a Dynatrac lock-in amplifier (Ithaco Model 393) together with a sine voltage from the signal generator as reference signal to the lock-in amplifier. The 393 lock-in amplifier as a vector voltmeter provides three outputs simultaneously available. They are the amplitude (A), the in-phase (real) component ($A \cos \phi$), and the quadrature (imaginary) component ($A \sin \phi$) where ϕ is the phase angle between the input signal and the reference signal to which the instrument is synchronized. A digital voltmeter or a recorder is used for the final reading.

The operational amplifier OA-2 (AD 515 KH) has a high dc open-loop gain ($\geq 4 \times 10^4$) and a very high input impedance (10^{15} Ω), and its bias current is less than 1.5×10^{-13} A; therefore, the $I-V$ converter can be used with values of the feedback resistor, R_F, approaching 10^{13} Ω in dc. However, when used in the ac mode and at frequencies above 5 Hz, the open-loop gain of the OA-2 is frequency dependent, and the open-loop gain rolls off along with the raise of the frequency. We have found that this is a primary factor for the limitation of the frequency response of the instrument. Due to this roll off, the input point, B, of the $I-V$ converter deviates virtually at ground potential. At that time, the effect of any capacitance between point B and ground as well as the input capacitance of OA-2 increases. For an $I-V$ converter, when the stray capacitance shunted at the feedback resistor, R_F, plus the effective input capacitance is C, the frequency response of this measuring circuit is limited by the time constant, R_FC, and the −3-dB point occurs at a frequency (f) (*9*) of

$$f = 1/2\pi R_F C \qquad (2)$$

In our case, when R_F and R_s are 1 MΩ, the stray capacitance between point B and ground as well as the input capacitance affects seriously the accuracy of impedance measurements for frequencies above 1 kHz (an example is shown in Figure 3b, see text below).

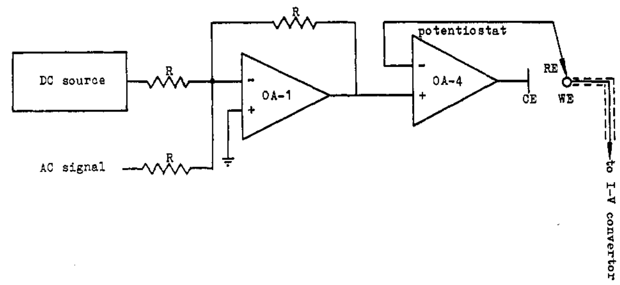

Figure 2. Additional circuit for polarization of the electrode: WE, working electrode; RE, reference electrode; CE, counter electrode.

To overcome this problem, a guarding technique, originally used for reduction of the shunt capacitance of the shield cable (*10*), was utilized here. A high-input impedance voltage follower is composed of the operational amplifier OA-3 (μA 748). Its input terminal connects to the point B, and the output terminal connects to the shield line of the $I-V$ converter input line and the metal case of OA-2. For the stability of the circuit, the power of the follower is supplied with a ±9-V battery group. This follower always holds the input point B and the shield line at the same level and phase of voltage; therefore no voltage drop arises across the insulation, and hence no leakage occurs. This reduces completely the effect of the capacitance between point B and ground and the input capacitance of OA-2.

At the same time, for reducing the stray shunt capacitances at the measuring (feedback) resistor, R_F, and the standard resistor, R_s, the fact that several smaller resistors in series compose the resistors R_F and R_s is utilized. Further, the resistors R_F and R_s were arranged at a distance above 10 cm away from any other circuit component. In order to shield the electronics and the measured cell from external electrical interference, they were put into a grounded $35 \times 45 \times 26.5$ cm^3 metallic shield box.

After these steps for reducing the effect of the stray capacitance between point B and ground have been taken, the instrument can measure the ac impedance at $R_F = R_s = 10$ MΩ in the frequency range from 3 Hz to 2 kHz without observable phase shift. With eq 2, an equivalent vestige capacitance of 0.8 pF in the complete system can be calculated. This clearly indicates the success.

Moreover, using this instrument with $R_F = R_s = 1$ MΩ and in a frequency range of the used lock-in amplifier from 1 Hz to 10 kHz, the phase shift deviates not more than 2° except at frequencies of 1 and 2 Hz. This makes it possible to use this instrument for automatic measurements of high ac impedance with very good accuracy and frequency resolution.

In order to allow the polarization of the electrode, an additional circuit shown in Figure 2 can be utilized. The sine alternating voltage from the divider network (see Figure 1) and the dc voltage from the dc source for the polarization of the electrode are added in the adding amplifier, which is composed of OA-1. Then the signal is fed into the potentiostat control input and is imposed between WE (working electrode) and RE (reference electrode) via generation of a suitable current output (dc plus ac) by the potentiostat control amplifier OA-4. Then the current from the measured cell is fed to the $I-V$ converter in Figure 1. When two potentiostats are used the four-electrode cell (two reference electrodes) control is possible.

CALIBRATION AND MEASUREMENT

All measurements were calibrated with a precision (0.1%) metal film resistor as the standard resistor, R_s. Because the $I-V$ converter was of the inversion phase type, for correction the toggle switch at the 393 lock-in amplifier is set to 180° out of phase. At the same time, for highly accurate measurements, the manual adjustment of the phase control vernier of the lock-in amplifier is used in order to offset the phase shift of the instrument circuit.

The calibration and measurement processes are as follows: activating the switch, K, to connect the standard resistor, R_s, in Figure 1, then adjusting the phase control vernier at the 393 lock-in amplifier to obtain the meter quadrature reading $A \sin \phi = 0$, reading off the meter amplitude reading, A_s (for

Table I. Exchange Current Densities of K^+-Selective PVC Membranes in KCl Solution (ac Impedance Method)

source	membrane composition, mg		KCl concn, M	charge transfer resistance (R_t), kΩ cm²	exchange current density (i_0), μA cm⁻²
ref 11	valinomycin	2.9			
	ester[a]	121.9	10^{-1}	1.5	17.2
	PVC	67.5			
ref 11	valinomycin	2.9			
	NaTPB[b]	0.8	10^{-1}	2.0	12.8
	ester	232.8			
	PVC	59.7			
ref 11	valinomycin	4.4			
	KTPB	1.1	10^{-1}	10.5	2.4
	ester	123.4			
	PVC	69.0			
this work	valinomycin	3.0			
	KTCPB[c]	0.7	10^{-3}	13.7	1.9
	DBP[d]	197.3			
	PVC	95.7			

[a] Bis(2-ethylhexyl)sebacic ester. [b] TPB, tetraphenylborate. [c] TCPB, tetrakis(4-chlorophenyl)borate. [d] DBP, dibutyl phthalate.

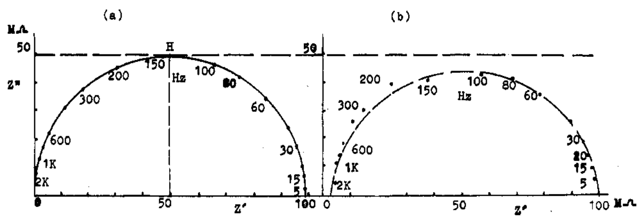

Figure 3. Measured complex impedance planes for a dummy cell consisting of a 100-MΩ resistor shunted by a 10-pF capacitor (a) using the guarding step and (b) without using the guarding step.

a pure resistor R_s, the quadrature component of ac impedance always equals null; hence the amplitude of ac impedance equals the in-phase component, i.e., $A_s = A_s \cos \phi$). After this, switch K is thrown to connect the measured cell, then the amplitude reading, A, together with the values of the in-phase component, $A \cos \phi$, and the quadrature component, $A \sin \phi$, are read off the meter. The impedance amplitude measured can be calculated by using the following equation:

$$Z = R_s A_s / A \tag{3}$$

and the real impedance component, Z', and the imaginary impedance component, Z'', are obtained from

$$Z' = Z \cos \phi = R_s A_s (A \cos \phi)/A^2 \tag{4}$$

$$Z'' = Z \sin \phi = R_s A_s (A \sin \phi)/A^2 \tag{5}$$

INSTRUMENT PERFORMANCE

The instrument performance for high ac impedance is demonstrated by measurements on a dummy cell consisting of a 100-MΩ metal film resistor shunted by a 10-pF ceramic capacitor. The feeback resistor, R_F, is chosen to be 10 MΩ and the excitation signal is 15–25 mV sine peak to peak. The complex impedance plane measured is a perfect semicircle as shown in Figure 3a. From the diameter the calculated value of R can be obtained as R = 98 MΩ, and in the highest point, H, of the semicircle there is

$$R = 1/2\pi f_h C \tag{6}$$

where f_h is the corresponding frequency of point H in Figure 3a. The calculated value of C can be obtained by using eq 6 and is found to be C = 11.2 pF. The values for R and C are in excellent agreement with the ceritified values and the error tolerance given.

For the sake of contrast, the ac impedance of the above-mentioned dummy cell (100 MΩ shunted by 10 pF) was also measured without using the guarding step at point B in Figure 1. In this condition the phase shift at a frequency of 2 kHz is in excess of 23°. Although the manual adjustment was taken, the measured result is a subsided and erroneous semicircle as shown in Figure 3b. Obviously, from this complex impedance plane the measured R and C cannot be accurately obtained.

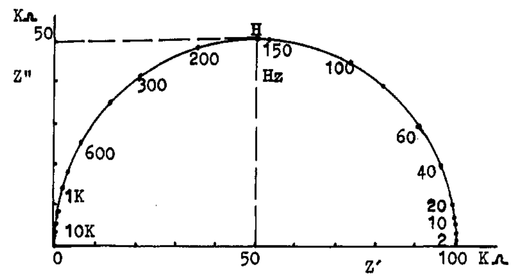

Figure 4. Measured complex impedance plane for a dummy cell consisting of a 100-kΩ resistor shunted by a 10-nF capacitor.

Another demonstration measurement was performed using a lower impedance range. A dummy cell was made of a 100-kΩ metal film resistor shunted by a 10-nF nylon capacitor. The measured result from 2 Hz to 10 kHz is shown in Figure 4. The calculated values of R and C are 99.5 kΩ and 9.95 nF, respectively.

The agreement with the certified values of the resistor and the capacitor is even better than in the first example.

For demonstration of the performance of the instrument on an actual electrochemical cell, the cell configuration shown in Figure 5 for the ac impedance research on ion-selective PVC membranes was used. It consists of a PTFE body (overall length 16.5 cm) with a cylindrical central bore (diameter 1.4 cm). The end plugs consist of a machined PTFE plug into which a plate (1 × 1 cm²) Ag/AgCl electrode is set. The cell also has two extra holes with plugs to facilitate three-electrode or four-electrode control. As an example, Figure 6 shows the measured result, the complex impedance plane from 1 Hz to 10 kHz, for a K^+-selective PVC membrane (based on valinomycin) in 10^{-3} M KCl solution at equilibrium potential. The excitation was 25 mV peak to peak. Obviously, the membrane bulk resistance, R_M (first semicircle), and the charge transfer resistance, R_T (second semicircle), can be clearly separated. From the R_T = 13.7 kΩ cm² the exchange current density, i_0 = 1.9 μA cm⁻², can be obtained. This was found to be close to the results (Table I) obtained by other researchers (*11*) who used a Solartron 1174 frequency response analyser (*6*) for the impedance measurement of K^+-selective PVC membranes.

ACCURACY

The accuracy of the standard resistor, R_s, is ±0.1%, plus the instrument error and the reading error; therefore, the error

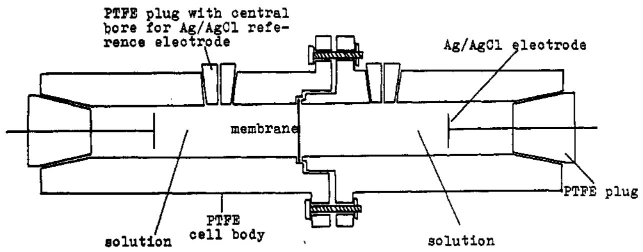

Figure 5. Configuration of the cell used for the ac impedance measurement of PVC membranes.

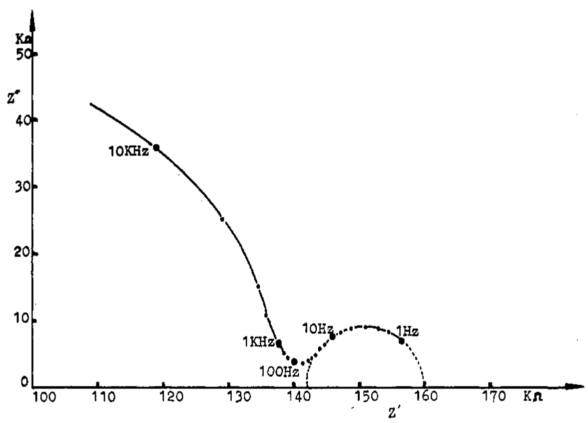

Figure 6. Measured complex impedance plane for a K^+-selective PVC membrane (based on valinomycin) in 10^{-3} M KCl solution.

of the measured impedance values is estimated to be less than ±0.5%.

CONCLUSIONS

By use of a lock-in amplifier together with some additional electronic aids, an instrument for the accurate measurement of very high ac impedances can be built. The construction of the circuitry, including application of a guard technique, eliminates successfully the effect of stray capacitances in the complete system to less than 0.8 pF. Demonstration measurements indicate that this instrumental setup can be used for very high ac impedance measurements (up to 100 MΩ) and still give highly accurate results. This instrument can be used for high-impedance membrane electrodes (PVC membrane, glass membrane) or in studies of the interface of two immiscible electrolyte solutions.

ACKNOWLEDGMENT

We are grateful to J. Andersson for correcting the English. We also thank the Alexander von Humboldt Foundation and the German "Fond der chemischen Industrie" for financial support.

Registry No. KTCPB, 14680-77-4; DBP, 84-74-2; PVC, 9002-86-2; KCl, 7447-40-7; valinomycin, 2001-95-8.

LITERATURE CITED

(1) MacDonald, D. D.; McKubre, M. C. H. *Mod. Aspects Electrochem.* **1982**, *14*, 61–150.
(2) Buck, R. P. *Ion-Sel. Electrode Rev.* **1982**, *4*, 3–74.
(3) Armstrong, R. D.; Bell, M. F.; Metcalfe, A. A. *Electrochemistry* **1978**, *6*, 98–121.
(4) Archer, W. I.; Armstrong, R. D. *Electrochemistry* **1978**, *7*, 157–201.
(5) Armstrong, R. D.; Bell, M. F.; Metcalfe, A. A. *J. Electroanal. Chem.* **1977**, *77*, 287.
(6) Gabrielli, C. *Identification of Electrochemical Processes by Freqency Response Analysis*; Solartron: Paris, 1980.
(7) Lang, J.; Schwitzgebel, G. *GIT Fachz. Lab.* **1984**, *28*(11), 997.
(8) Bentz, A. J.; Sandifer, J. R.; Buck, R. P. *Anal. Chem.* **1974**, *46*(4), 543–547.
(9) Cath, P. G.; Peabody, A. M. *Anal. Chem.* **1971**, *43*(11), 91A.
(10) Aitchison, R. E.; Brown, T. J. *Electron. Eng.* **1976**, *48*, 23.
(11) Armstrong, R. D.; Covington, A. K.; Evans, G. P. *J. Electroanal. Chem.* **1983**, *159*, 33–40.

RECEIVED for review September 3, 1985. Accepted February 24, 1986.

Theory of Sedimentation Hyperlayer Field-Flow Fractionation

Mark R. Schure,[1] Karin D. Caldwell, and J. Calvin Giddings*

Department of Chemistry, University of Utah, Salt Lake City, Utah 84112

The theory of a new separation technique, sedimentation hyperlayer field-flow fractionation, is presented. This technique differs from conventional field-flow fractionation methods in that the solute zone is focused into a thin sheet by the opposing forces of centrifugal acceleration and buoyancy in a density gradient. Emphasis in this paper is given to the nature and distribution of the density modifier and its effect on the velocity profile, the zone concentration profile, zone spreading, selectivity of separation, and the conditions needed to achieve practical separations that approach the theoretical limit. Both sample size and dilution are shown to be factors requiring consideration for achieving practical separations.

In recent years, the family of separation techniques known as field-flow fractionation (FFF) has been found to be a powerful and at the same time a very broad approach for resolving mixtures of macromolecules or particles into their components (*1*). The wide applicability of the FFF technique stems from the numerous choices in field type, field strength, carrier type (aqueous, nonaqueous, etc.), flow conditions, programming options, and channel dimensions.

In FFF, separations are carried out in a single phase in which an externally applied (and totally controllable) field transports components into regions of different flow velocities near the wall of a flow channel. Here they are displaced differentially by the nonuniform flow, and they thus emerge separately. The basic mechanism of transport is illustrated diagramatically in Figure 1A.

Most applications of FFF have been carried out in ribbonlike channels whose geometry can be characterized as the space between infinite parallel plates; i.e., the flow chamber has a breadth far exceeding its thickness. The carrier fluid flows under laminar conditions, and the superimposed field acts uniformly in a direction perpendicular to the flow.

In all the normal FFF methods, excluding steric FFF (*2*, *3*), the sample particles form an exponential cloud against one

[1] Present address: Digital Equipment Corp., 1 Iron Way, MR02-4/E33, Marlborough, MA 01752.

